

Mid-IR quantum cascade laser mode coupling in hollow-core, fiber-optic waveguides with single-mode beam delivery

P. Patimisco^{*a,b}, A. Sampaolo^{a,b}, J. M. Kriesel^c, G. Scamarcio^b, and V. Spagnolo^b

^aRice University, Department of Electrical and Computer Engineering, 6100 Main Street, Houston, TX 77005, USA;

^bDipartimento Interateneo di Fisica, Università e Politecnico di Bari, CNR-IFN UOS BARI, Via Amendola 173, Bari, Italy;

^cOpto-Knowledge Systems, Inc. (OKSI), 19805 Hamilton Ave., Torrance CA, USA 90502-1341;

ABSTRACT

We report a theoretical and experimental study of laser coupling in hollow-core, fiber-optic waveguides with small-bore diameters of $d=200\text{ }\mu\text{m}$. For the experiments we utilized three mid-infrared quantum cascade lasers with different emission wavelength, which were coupled into the waveguides using lenses with focal lengths in the range 25-76 mm. Measurements of the output beam profiles and propagation losses were obtained as a function of the coupling conditions. With appropriate coupling parameters, single mode beam delivery can be obtained for all laser wavelengths, ranging from $\lambda \sim 5.4$ to $10.5\text{ }\mu\text{m}$.

Keywords: fiber-optic, hollow-core waveguide, quantum cascade laser, optical coupling.

1. INTRODUCTION

The mid-infrared (mid-IR) spectral region of 5 to $10\text{ }\mu\text{m}$ is currently of growing interest because the development of a new generation of laser sources with high potentialities for several applications, including for example laser surgery, infrared spectroscopy, thermal imaging, sensing and infrared countermeasures. For many of these applications, it is strongly desirable to employ single-mode fibers for high-optical quality beam laser delivery. Thus, there is a great interest in the possibility to realize low-loss single-mode fibers operating in this spectral range. Towards this goal, several avenues have been explored with chalcogenide glasses, fluoride, polycrystalline and tellurite fibers [1-3]. Whilst low attenuation values have been achieved (e.g. 0.45 dB/km [3]), a mid-IR solid-core fiber has not yet been able to provide a combination of durability, bend insensitivity, modal quality and power handling in the whole mid-IR spectral range as offered by silica-based fibers in the near-IR.

Hollow core waveguides (HCWs) where the majority of the light is guided in air, minimizing loss contributions from material absorption offer an attractive alternative [4]. Indeed, the guided mode in these fibers is strongly confined within the hollow core, greatly reducing the effect of the solid material on the fiber's optical properties and liberating its performance from the material constraints. The HCWs structure is composed of a hollow glass capillary tube with a metallic/dielectric structure deposited inside the bore [4]. The bore size, typical below 1 mm, determines the overall losses and mode quality, whereas the thickness of the dielectric layer determines the spectral response [5]. Guidance in a hollow core also offers high coupling efficiency, a higher damage threshold, no back reflection, no cladding modes, high energy/power handling capabilities and additional functionalities leading to further applications such as gas sensing and quantum optics [6, 7]. This is particularly of interest in the mid- to far-IR where the fundamental vibrational lines of molecular species lie; these resonances are inherently stronger than those in the near IR, indicating great potentialities for high precision spectroscopy at ultra-low pressures and gas sensing with faster response times [8, 9]. Hollow core silica-based fibers with a bore diameter of $d = 300\text{ }\mu\text{m}$ have recently been reported to deliver optical guidance in the range 8-11 μm with a single spatial mode [10, 11].

*pietro.patimisco@uniba.it; phone 39 080 544-2373; fax 39 080 544-2219

It has been predicted that single-mode beam profile output can be obtained when the bore diameter d is lower than 40 times the light wavelength [12], so in order to obtain single-mode propagation down to $\lambda = 5 \mu\text{m}$, a HCW with $d \sim 200 \mu\text{m}$ should be employed.

In this work, we present highly flexible small-bore hollow waveguides with a bore diameter of $200 \mu\text{m}$ consisting of a silver (Ag) and silver iodine (AgI) coating deposited inside silica tubing, with lengths of 15 cm and 50 cm. We demonstrate the possibility to employ these HCWs for delivering of laser radiation in the mid-IR spectral region of 5 to $10 \mu\text{m}$ with single spatial mode output profile and low propagation losses. Using a beam profiler we studied the output intensity distributions of hollow waveguides coupled with continuous-wave quantum cascade lasers (QCLs) emitting at $5.2 \mu\text{m}$, $6.4 \mu\text{m}$ and $10.5 \mu\text{m}$. We investigated also the effect of launch conditions on the mode quality of the output beam profile and on the transmission properties of these HCWs, in both straight and bent configurations. Different coupling conditions between the lasers beam and the waveguides entrance were realized using mid-infrared lenses with different focal lengths in the range 25-76 mm. For a fiber length of 15 cm, we reached losses down to 1.55 dB at $5.4 \mu\text{m}$, 1.32 dB at $6.2 \mu\text{m}$, and 0.86 dB at $10.5 \mu\text{m}$, by choosing the best coupling conditions between the QCL and the HCW.

2. EXPERIMENTAL APPROACH

In this section, we present the experimental setup and methodology used to measure the beam quality and to study the beam properties of light exiting the HCWs. The setup is shown in Fig. 1.

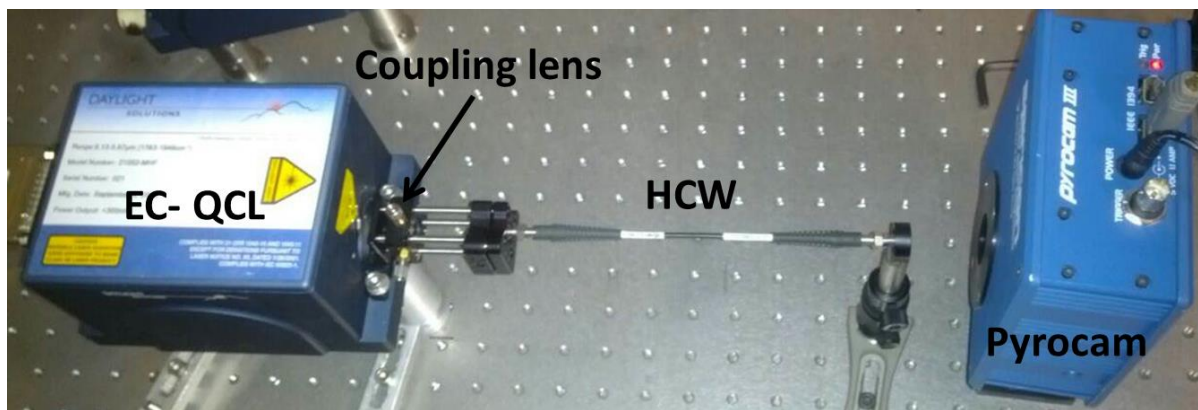


Figure 1. A picture of the experimental setup. The laser beam is focused at the waveguide entrance by using a coupling lens. The beam profile at the waveguide exit is acquired with an infrared pyrocamera. EC-QCL – External-Cavity Quantum Cascade Laser; HCW – Hollow-Core Waveguide.

Three commercial mid-IR quantum cascade laser (QCL) sources (Daylight Solutions Inc., San Diego, CA, USA, model #21052-MHF, #21106-MHF, #21062-MHF) based on an external-cavity configuration were used to measure the attenuation of the hollow waveguides, the optical mode profile at the waveguide exit and to examine the influence of the input launch conditions on the beam propagation through the fiber. The selected emission wavelengths are $5.4 \mu\text{m}$, $6.2 \mu\text{m}$ and $10.5 \mu\text{m}$. The average optical powers measured at the exit of the QCL using a power meter were 115 mW at $5.4 \mu\text{m}$, 80 mW at $6.2 \mu\text{m}$, and 56 mW at $10.4 \mu\text{m}$. The beam quality at the output of a fiber depends on the fiber properties, but also may vary with the launch beam conditions including beam quality and position and angle of the input beam relative to the fiber axis [13]. For this reason, a coupling lens with a diameter of $1/2''$ attached to a translation mount was used to focus the collimated laser beam into the HCW entrance. The HCW was held in another mount, which allowed for tilt adjustments of the position of the HCW entrance with respect to the focused laser beam. The optimal fiber input alignment was found by maximizing the output fiber exit. This alignment was obtained by careful tuning the positions of both the lens and the HCW entrance. In order to record the mode profile in the far field condition, a pyrocamera (Pyrocam III, Ophir Spiricon) with pixel sizes of $0.085 \times 0.085 \text{ mm}$ was mounted at distances $\geq 2.5 \text{ cm}$ from the HCW output. We employed two different HCWs with metallic (Ag)/dielectric (AgI) circular cross-section internal coatings, a bore size of $d = 200 \mu\text{m}$, and lengths of 15 cm and 50 cm. Fabrication of the HCWs is accomplished using a wet

chemistry process developed by Harrington et al. [4-5]. It consists of depositing a reflective silver (Ag) layer followed by a dielectric silver iodide (AgI) layer inside a glass tube. The spectral properties of the hollow fibers are determined by the thickness of the AgI dielectric layer, which is typically about 0.1 μm to 1.0 μm thick [5]. By producing a hollow fiber with a specific dielectric thickness layer, the transmission spectrum of the waveguides can be tailored for different spectral wavelength ranges. The actual thickness of the AgI layer, calculated from the Fourier transform infrared spectrometer, is about 0.56 μm .

The theory of the propagation of light through cylindrical hollow metallic waveguides was first proposed by Marcatili and Schmeltzer [14] and then improved by Miyagi and Kawakami [15], which included the influence of the dielectric layer on the propagation losses. They derived an expression of the attenuation coefficient to calculate losses for HE_{1m} modes that propagate within hollow waveguides when a Gaussian beam is coupled into the HCW. The amount of the light energy entering a HCW can be referred to as the coupling efficiency. The value of the coupling coefficient is dependent on the spatial distribution of the light at the waveguide entrance and the waveguide mode profile. Hence, the coupling efficiency can be computed from the squared modulus of the overlap integral between the input Gaussian mode with a beam waist ω_0 at the waveguide entrance, and the HE_{1m} waveguide modes, which can be approximated by the zero-order Bessel function [13]. As result, the power-coupling coefficient for the various modes is a function of the ratio of ω_0 and the bore radius of the waveguide and essentially depends by how much the focused beam fills the hollow bore. Minimal loss condition is achieved when this ratio is about 0.64, so it is mandatory to optimize the laser beam coupling into the HCW by using appropriate focal length lenses to approximate this ratio. The transmitted intensity I by HCW with a length of L has been calculated using [13] the following equation:

$$I = \sum_m \eta_{1m} e^{-2\alpha_{1m}L} \quad (1)$$

The focused beam waist is related to the f-number of the coupling lens as:

$$f_{\#} = \frac{\pi\omega_0}{2\lambda} \quad (2)$$

In our experiment, by employing lenses with different focal lengths, we varied the properties of the incoming beam, i.e., we achieved different waist sizes at the HCW entrance. We characterized the size of the launch both with the fraction ω_0/a , where “a” is the radius of the HCW, and the f-number which is directly related to the lens numerical aperture NA by $f_{\#} \approx 1/2\text{NA}$. Figures 2a-c show the output beam profile of the three employed QCL sources measured while shining the collimated beams on the camera.

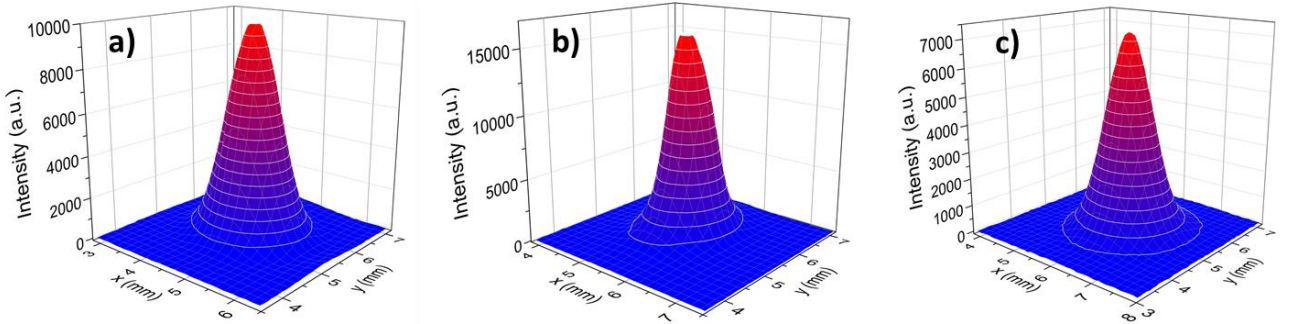


Figure 2a-c. Far field spatial intensity distributions of the QCL emitting at 5.4 μm (a), QCL emitting at 6.2 μm (b) and QCL emitting at 10.5 μm (c). The beam profile has been measured by locating the pyro-camera at a distance of about 2.5 cm away from the QCL output.

The intensity distribution profiles exhibit single-mode Gaussian-like beam output, as expected for a standard edge emitting QCLs, with beam diameters D slowly varying one from the other ($D = 2.36$ mm for $\lambda = 5.4$ μm , $D = 2.66$ mm for $\lambda = 6.2$ μm , and $D = 2.4$ mm for $\lambda = 10.5$ μm).

3. OUTPUT BEAM PROFILES AT THE WAVEGUIDE EXIT

All three QCL sources have been used to measure the attenuation of the hollow waveguides and to examine the influence of the input launch conditions on the loss behavior. The QCL beam is coupled into the waveguide via a focusing lens that

guides the beam directly in the center of the HCW, in straight condition. The investigation of the QCL-HCW optical coupling requires the use of lenses with different focal lengths, in order to explore the propagation losses and the output mode quality at different ω_0/a values. Input spot size smaller than the waveguide bore diameter reduces the amount of energy blocked by the waveguide wall, a critical point for high-power applications [16]. Figures 3a-i show the far field spatial intensity distribution obtained in a straight line condition at the exit of a 15 cm-long HCW, by using coupling lenses with focal length of $f = 25$ mm (Fig. 3a, d, g), $f = 40$ mm (Fig. 3h), $f = 50$ mm (Fig. 3b, e, i) and $f = 76$ mm (Fig. 3c, f), at $\lambda = 5.4 \mu\text{m}$ (Figs. 3a-c), $\lambda = 6.2 \mu\text{m}$ (Figs. 3d-f), and $\lambda = 10.5 \mu\text{m}$ (Figs. 3g-i). In each panel, f-numbers (calculated by using Eq. 2) and ratios ω_0/a are also reported. In this investigation, the pyro-camera was placed at the output of the waveguide with the sensor located about 2.5 cm from the waveguide output. No additional imaging optics were used.

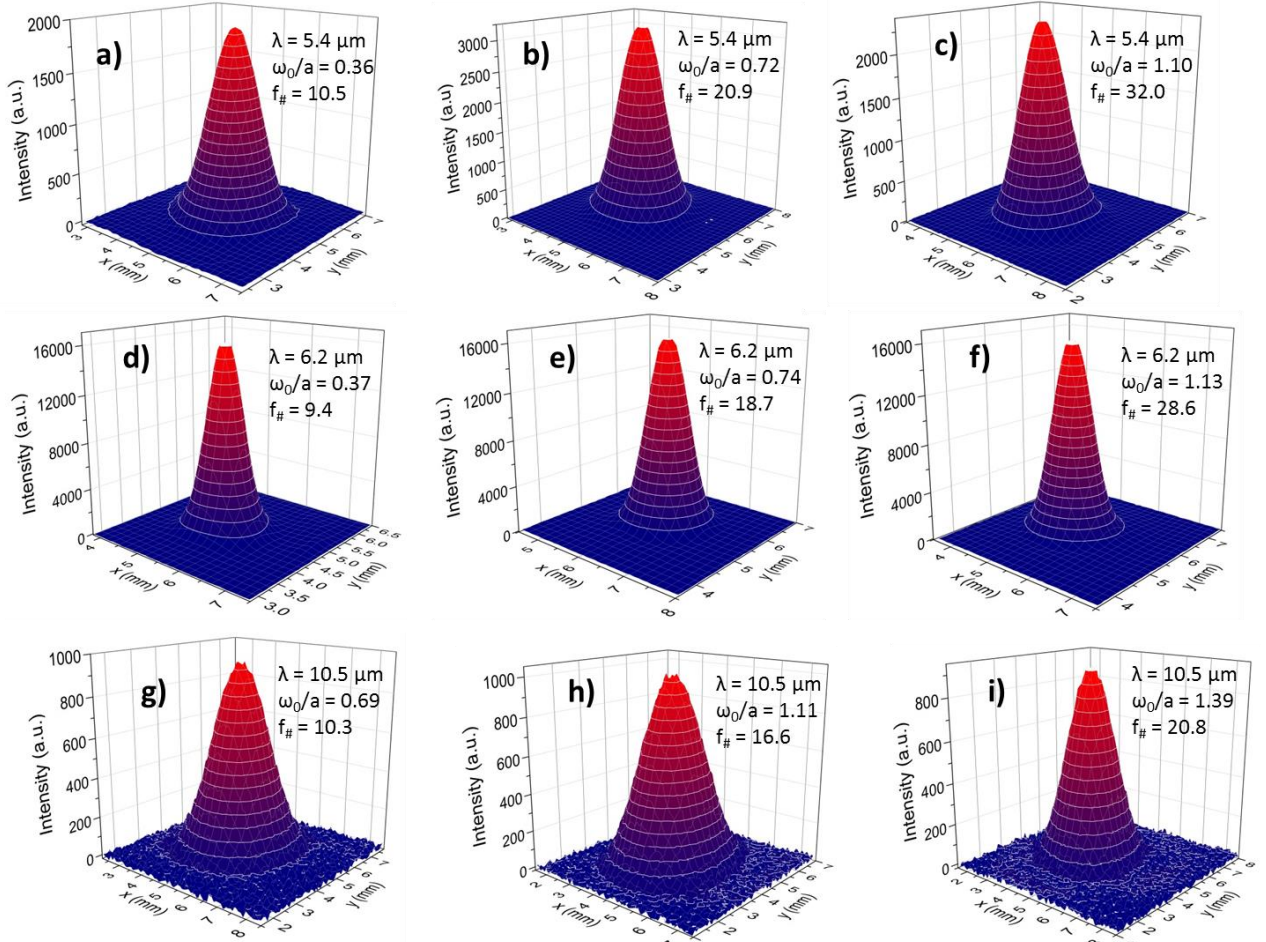


Figure 3a-i. Output beam profiles upon exiting at 15 cm-long HCW, employing coupling lenses with focal lengths: $f = 25$ mm ((a), (d), and (g)), $f = 40$ mm (h), $f = 50$ mm ((b), (e), and (i)) and $f = 76$ mm ((c), (f)), for $\lambda = 5.4 \mu\text{m}$ ((a)-(c)), $\lambda = 6.2 \mu\text{m}$ ((d)-(f)) and $\lambda = 10.5 \mu\text{m}$ ((g)-(i)). The beam profiles have been obtained with the experimental scheme illustrated in Fig. 1. The distance between the fiber output and the pyrocamera detector has been fixed to ~ 2.5 cm.

The 2-D far field acquisitions demonstrate that HCWs with bore sizes of $200 \mu\text{m}$ allow single-mode propagation of laser beam at $\lambda = 5.4 \mu\text{m}$, $\lambda = 6.2 \mu\text{m}$ and $\lambda = 10.5 \mu\text{m}$, also with fiber length down to 15 cm. Similar results have been obtained for the HCW with length of 50 cm. The input face of the fiber was positioned at the waist of the incoming beam to a precision of less than 1 mm. Experimentally we verified that as long as the separation distance between the fiber entrance and the beam waist position was less than Rayleigh range, $z_R = \pi\omega_0^2/\lambda$, the output beam quality was almost unchanged, instead as this separation distance increased to more than z_R the output beam quality decreased. For $0.36 \leq$

$\omega_0/a \leq 1.39$, our experiments have shown that the a single mode beam output quality is preserved, so even though the coupling conditions are significantly different, the modal purity is good, resulting in a beam shape matched to the hybrid HE_{11} mode in almost all investigated coupling configurations.

The output divergence angle characterizes the diffraction of light leaving the waveguide and depends on the modes propagating in the guide as well as the bore size. The HE_{1m} modes will couple to free-space modes with a half-angle beam divergence given by [4]:

$$\theta_{1m} = \frac{u_{1m}\lambda}{2\pi a} \quad (3)$$

The lowest order mode gives the smallest beam divergence, while θ_{1m} rapidly increase for the higher-order modes [4]. The beam divergence at the HCW end face has been estimated by measuring the radial distances at which the light intensity drops to $1/e^2$ of its maximum central value, from the far field scans acquired at different distances from the fiber output. Each 2D-scan was then fit to a Gaussian function, and the parameter corresponding to the $1/e^2$ radius of the Gaussian was recorded as the radial value [7]. Figure 4 shows radial values extracted at different positions of the pyro-camera starting from $z_0 \sim 2$ cm far from the 15cm-long HCW output, by using the QCL emitting at $6.2 \mu\text{m}$, for the best coupling condition $f = 50$ mm (corresponding to $\omega_0/a = 0.74$).

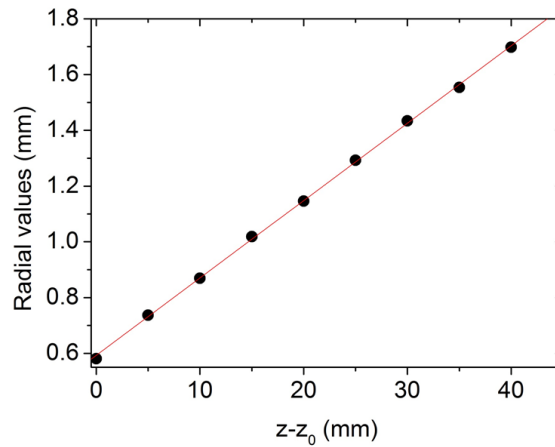


Figure 4. Radial values at which the light intensity drops to $1/e^2$ of its maximum central value of the beam profiles extracted at different positions of the pyro-camera, starting from $z_0 \sim 2$ cm away from the 15cm-long HCW output. The optical coupling between the QCL beam at $6.2 \mu\text{m}$ and the waveguide entrance were obtained using a lens with focal lengths $f = 50$ mm, giving $\omega_0/a = 0.74$.

The half-angle beam divergence is extracted from the linear fit to the data. Similar approach has been adopted for the output divergence measurements at $\lambda = 5.4 \mu\text{m}$ (with the coupling lens between the QCL and the HCW of $f = 50$ mm, corresponding to $\omega_0/a = 0.74$) and $\lambda = 10.5 \mu\text{m}$ (with coupling lens of $f = 25$ mm, corresponding to $\omega_0/a = 0.69$). In table 1 are listed the calculated beam divergences θ_{11} obtained by using Eq. 3 with $u_{11} = 2.4048$, and the related measured values θ_{meas} .

Table 1. Calculated θ_{11} values obtained by using Eq. 3 and measured half-angle beam divergence values for $\lambda = 5.4 \mu\text{m}$, $\lambda = 6.2 \mu\text{m}$ and $\lambda = 10.5 \mu\text{m}$, employing a coupling lens with focal length of 50 mm for $\lambda = 5.4 \mu\text{m}$ and $\lambda = 6.2 \mu\text{m}$, and a coupling lens with focal length of 25 mm for $\lambda = 10.5 \mu\text{m}$.

Wavelength (μm)	θ_{11} (mrad)	θ_{meas} (mrad)
5.4	20.6	25.0
6.2	23.9	26.5
10.5	40.2	42.3

A comparison between the measured values θ_{meas} and the calculated θ_{11} further confirms single-mode propagation of the laser beam in the hollow waveguide for all three investigated wavelengths and good mode coupling between the laser-input optical mode and the waveguide lowest-loss HE_{11} mode.

4. PROPAGATION LOSSES

Propagating losses in hollow waveguides are highly dependent on the launch conditions, i.e., the ratio ω_0/a . Theoretically up to ~100% of power coupling efficiency of an incident Gaussian beam to the lowest-loss HE_{11} mode can be obtained [13]. By changing the value of the ratio ω_0/a and maximizing the output power it is possible to couple most of the light in the HE_{11} mode. The propagation losses at different coupling conditions can be determined by making two measurements. First we measured the optical power I_0 at the waveguide entrance, then the light is coupled into the fiber and the optical power I_s at the output-end of the fiber is measured [7]. Absolute values of the losses of the excited mode of the straight waveguide were determined by using the following equation:

$$Losses(dB) = 10 \log_{10} \left(\frac{I_0}{I_s} \right) \quad (4)$$

Table 2 shows the propagation losses of 15 cm and 50 cm long HCWs measured as a function of the ratio ω_0/a for all three investigated wavelengths, at different launching conditions described above. Also, included in Table 2 for comparison are the theoretical losses for these waveguides, calculated using Eqs. 1 and 4, assuming that the HE_{11} and higher-order modes up to $m = 5$ propagate. It is particularly important to sum over all possible modes when calculating theoretical losses for waveguides, since many higher order modes can be excited.

Table 2. Experimental losses and calculated propagation losses by using Eqs. 1 and 4, for $\lambda = 5.4 \mu m$, $\lambda = 6.2 \mu m$ and $\lambda = 10.5 \mu m$ at different coupling conditions.

$\lambda (\mu m)$	ω_0/a	L = 15 cm		L = 50 cm	
		Theoretical Losses (dB)	Experimental Losses (dB)	Theoretical Losses (dB)	Experimental Losses (dB)
5.4	0.36	0.73	1.86	1.76	3.66
	0.72	0.54	1.55	1.05	2.75
	1.1	1.39	2.45	1.95	3.78
6.2	0.37	0.78	1.46	1.88	2.99
	0.74	0.61	1.32	1.20	2.21
	1.13	1.49	2.16	2.15	3.28
10.5	0.69	0.76	0.86	1.89	2.11
	1.11	1.71	1.89	2.90	3.18
	1.39	2.26	2.62	3.48	4.10

The measured losses are higher than the calculated values, especially at shorter wavelengths ($\lambda = 5.4 \mu m$ and $\lambda = 6.2 \mu m$). These discrepancies between theoretical and experimental values increases for the longer HCWs. As a possible explanation for this can be the presence of additional scattering losses due to the structural imperfections, mainly inner surface roughness of the guides, that affect the transmission losses at shorter wavelengths [17, 18]. In addition, it is evident from the data in Table 2 that the inner surface roughness almost does not affect the loss at $10.5 \mu m$. Matsuura et al. [17], using a ray-optics approach, showed that these scattering losses decrease with wavelength as $1/\lambda^2$. In Fig. 5, the measured losses and theoretical values was plotted as a function of $1/\lambda^2$ for a 15 cm-long HWC at $\lambda = 5.4 \mu m$, $\lambda = 6.2 \mu m$ and $\lambda = 10.4 \mu m$ when the ratio ω_0/a equals to 0.72, 0.74 and 0.69 (see Table 2), respectively, i.e. the best achievable conditions in terms of output mode quality. The results support our assumption that an additional contribution to the total losses originates from light scattering due to surface roughness of the inner HCW metallic layer. This contribution increases as the wavelength radiation decreases.

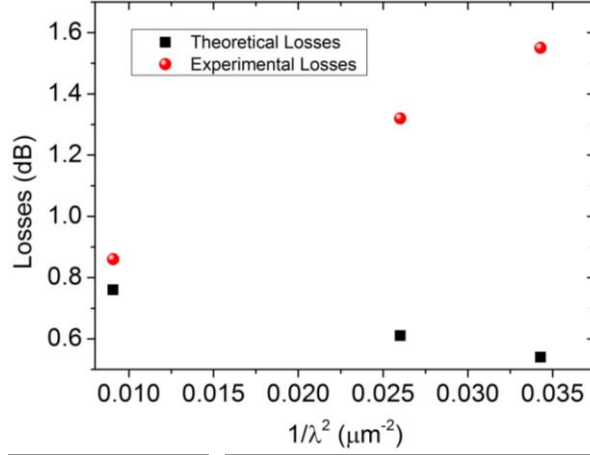
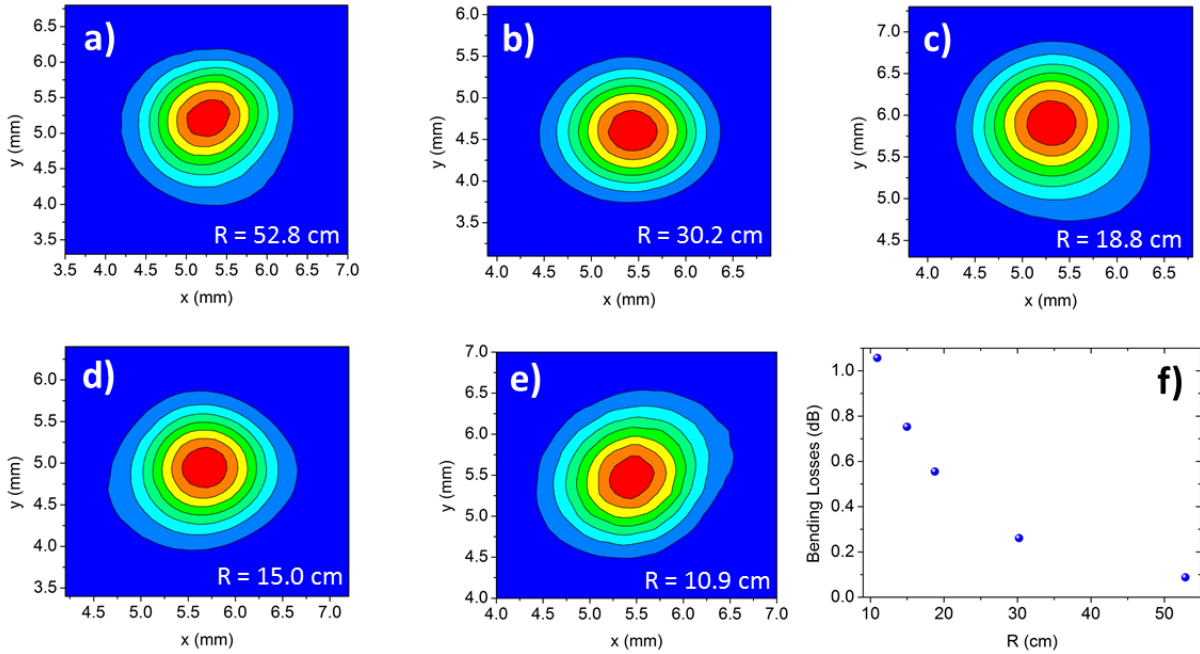


Figure 5. Theoretical (■) and experimental (●) losses measured for $\lambda = 5.4 \mu\text{m}$, $\lambda = 6.2 \mu\text{m}$ and $\lambda = 10.4 \mu\text{m}$ for a 15 cm-long HWC plotted as a function of $1/\lambda^2$.

5. BENDING LOSSES

The length of the waveguide used in the measurement of the bending losses is 50 cm. Input and output ends of the guides are kept straight, and a center part with a fixed length of 25 cm is bent to a uniform bending radius. We have performed tests to consider possible changes in beam quality and total losses at different radii of curvature. Figure 6a-e report output beam profiles acquired at different curvatures when the QCL emitting at $5.4 \mu\text{m}$ is coupled with 200- μm HCW with the coupling lens of $f = 50 \text{ mm}$.

Figure 6a-f. Output beam profiles ((a)-(e)) acquired $\sim 2.5 \text{ cm}$ away for 50 cm-long HCW for $\lambda = 5.4 \mu\text{m}$ with the coupling lens of $f = 50 \text{ mm}$, when the HCW is bent to uniform bending radii. (f) Measured bending losses plotted as a function of the radius of curvature.



The output beam profiles remain single-mode with slight spatial distortions even when the waveguide is bent into 10.9 cm of radius of curvature. Similar behavior has been observed with $\lambda = 6.2 \mu\text{m}$ and $10.5 \mu\text{m}$. In Fig. 6f bending losses as

a function of the radius of curvature are reported. The losses shown here are quite low, less than 1.1 dB, even when the waveguide was bent into 10.9 cm-radius. The magnitude of these losses depends largely on the quality of the inner surface [19, 20].

6. CONCLUSIONS

Hollow metallic and dielectric coated glass waveguides with bore diameters as small as 200 μm have been developed and tested to provide efficient single-mode transmission in the broad wavelength interval 5.4-10.5 μm into the mid-IR spectral range. The waveguide optical properties depend on the laser launch conditions into the waveguide, and propagation losses have been predicted by using fundamental waveguide theory. The waveguide with a length of 50 cm exhibits straight losses down to 2.75 dB at 5.2 μm when proper coupling conditions between the laser source and the waveguide are adopted, and the losses increases of 1.1 dB under bending with a radius of curvature down to 10.9 cm. A discrepancy between the measured straight losses and the theoretical values was measured and attributed to scattering losses, i.e. the interaction of light with the rough imperfect inner surface into the hollow waveguide. Our study shows that this contribution to total losses is higher at shorter wavelengths (5.4-6.2 μm) and becomes almost negligible at 10.5 μm . Finally, we demonstrated that small-bore waveguides have advantages in terms of single-mode propagation and low-losses in a wide mid-IR spectral interval, and can be used to delivery laser beam for some surgical and industrial applications, such as cutting and ablation, in which the beam quality nearly to a Gaussian output mode is required.

ACKNOWLEDGEMENTS

The authors gratefully acknowledge financial support from three Italian research projects: PON01 02238, PON02 00675 and PON02 00576.

REFERENCES

- [1] Sanghera, J. S., and Aggarwal, I. D., "Active and passive chalcogenide glass optical fibers for IR applications: a review," *Journal of Non-Crystalline Solids*, 256, 6-16 (1999).
- [2] Sanghera, J. S., Shaw L. B., and Aggarwal, I. D., "Applications of chalcogenide glass optical fibres," *C. R. Chimie*, 5, 873-883 (2002).
- [3] Carter, P. W., Moore, S.F., Szebesta, M. W., Williams, D., Ranson, J. R., and France, D., "Low Loss Fluoride Fibre by Reduced Die Casting," *Electron. Lett.*, 26, 2115-2117 (1990).
- [4] J.A. Harrington, [Infrared Fibers and Their Applications], SPIE Press, Bellingham, WA (2004).
- [5] Bledt, C. M., Harrington, J. A., and Kriesel, J. M., "Loss and modal properties of Ag/AgI hollow glass waveguides," *Appl. Opt.* 51, 3114-3119 (2012).
- [6] Patimisco, P., Spagnolo, V., Vitiello, M. S., Tredicucci, A., Scamarcio, G., Bledt, C. M., and Harrington, J. A., "Coupling external cavity mid-IR quantum cascade lasers with low loss hollow metallic/dielectric waveguides," *Appl. Phys. B* 108, 255-260 (2012).
- [7] Patimisco, P., Spagnolo, V., Vitiello, M. S., Tredicucci, A., Scamarcio, G., Bledt, C. M., and Harrington, J. A., "Low-Loss Hollow Waveguide Fibers for Mid-Infrared Quantum Cascade Laser Sensing Applications," *Sensors* 13, 1329-1340 (2013).
- [8] Spagnolo, V., Patimisco, P., Borri, S., Scamarcio, G., Bernacki, B. E., and Kriesel, J., "Part-per-trillion level SF₆ detection using a quartz enhanced photoacoustic spectroscopy-based sensor with single-mode fiber-coupled quantum cascade laser excitation," *Opt. Lett.*, 37, 4461-4463 (2012).
- [9] Spagnolo, V., Patimisco, P., Borri, S., Scamarcio, G., Bernacki, B. E., and Kriesel, J., "Mid-infrared fiber-coupled QCL-QEPAS sensor," *Appl. Phys. B* 112, 25-33 (2013).
- [10] Siciliani de Cumis, M., Viciani, S., Borri, S., Patimisco, P., Sampao, A., Scamarcio, G., De Natale, P., D'Amato, F., and Spagnolo, V., "A widely-tunable mid-infrared fiber-coupled quartz-enhanced photoacoustic sensor for environmental monitoring," *Opt. Express* 22, 28222-28231 (2014).
- [11] J. Kriesel, G. M. Hagglund, N. Gat, V. Spagnolo, and P. Patimisco, "Spatial mode filtering of mid-infrared (mid-IR) laser beams with hollow core fiber optics," *Proc. SPIE* 8993, 89930V-1-9 (2014).
- [12] J.M. Kriesel, N. Gat, B.E. Bernacki, R.L. Erikson, B.D. Cannon, T.L. Myers, C.M. Bledt, and J.A. Harrington, "Hollow Core Fiber Optics for Mid-Wave and Long-Wave Infrared Spectroscopy," *Proc. SPIE* Vol 8018, 80180V (2011).

- [13] R. Nubling and J.A. Harrington, "Launch conditions and mode coupling in hollow glass waveguides," *Opt. Eng.* 37, 2454–2458 (1998).
- [14] Marcantili, E. A. J., and Schmeltzer, R.A., "Hollow metallic and dielectric waveguides for long distance optical transmission and lasers," *Bell. Syst. Tech. J.* 43, 1783–1809 (1964).
- [15] Matsuura Y., and Miyagi, M., "Hollow Optical Fibers for Ultraviolet and Vacuum Ultraviolet Light," *IEEE Journal of Selected Topics in Quantum Electronics* 10, 1430-1434 (2004).
- [16] C. M. Bledt, D. V. Kopp, J. A. Harrington, S. Kino, Y. Matsuura and J. M. Kriesel, "Investigation of tapered silver / silver halide coated hollow glass waveguides for the transmission of CO₂ laser radiation", *Proc. SPIE* Vol. 8218, 821802 (2012).
- [17] Matsuura, Y., Saito, M., Miyagi, M., and Hongo, A., "Loss characteristics of circular hollow waveguides for incoherent infrared light," *J. Opt. Soc. Am. A* 6, 423–427 (1989).
- [18] Rabii, C. D., Gibson, D. J., and Harrington, J. A., "Processing and characterization of silver films used to fabricate hollow glass waveguides," *Appl. Opt.* 38, 4486- 4493 (1999).
- [19] Matsuura, Y., Abel, T., and Harrington, J. A., "Optical properties of small-bore hollow glass waveguides," *Appl. Opt.* 34, 6842-6847 (1995).
- [20] Miyagi, M., "Bending losses in hollow and dielectric tube leaky waveguides," *Appl. Opt.* 20, 1221- 1229 (1981).